Plant Physiol. (1997) 115: 1089–1099

Apoplasmic and Protoplasmic Water Transport through the Parenchyma of the Potato Storage Organ

Werner Michael, Alexander Schultz, Anatoli B. Meshcheryakov, and Rudolf Ehwald*

Institut für Biologie, Mathematisch-Naturwissenschaftliche Fakultät I, Humboldt-Universität zu Berlin, Invalidenstrasse 42, 10115 Berlin, Germany (W.M., A.S., R.E.); and Timiryasev-Institute of Plant Physiology, Russian Academy of Sciences, 127 276 Moscow, Botanicheskaya Ulica, 35, Russia (A.B.M.)

Stationary volume fluxes through living and denatured parenchyma slices of the potato (*Solanum tuberosum* L.) storage organ were studied to estimate the hydraulic conductivity of the cell wall and to evaluate the significance of water transport through protoplasts, cell walls, and intercellular spaces. Slices were placed between liquid compartments, steady-state fluxes induced by pressure or concentration gradients of low- and high-molecular-mass osmotica were measured, and water transport pathways were distinguished on the basis of their difference in limiting pore size. The protoplasts were the dominating route for osmotically driven water transport through living slices, even in the case of a polymer osmoticum that is excluded from cell walls. The specific hydraulic conductivity of the cell wall matrix is too small to allow a significant contribution of the narrow cell wall bypass to water flow through the living tissue. This conclusion is based on (a) ultrafilter coefficients of denatured parenchyma slices, (b) the absence of a significant difference between ultrafilter coefficients of the living tissue slices for osmotica with low and high cell wall reflection coefficients, and (c) the absence of a significant interaction (solvent drag) between apoplasmic permeation of mannitol and the water flux caused by a concentration difference of excluded polyethylene glycol. Liquid-filled intercellular spaces were the dominating pathways for pressure-driven volume fluxes through the parenchyma tissue.

In textbooks and reviews (Anderson, 1976; Läuchli, 1976; Pitman, 1977), the nonspecialized apoplast is usually considered more permeable to water than the protoplast or the symplast. However, several authors (Myers, 1951; Tyree, 1968, 1973; Molz and Ilkenberry, 1974; Newman, 1976; Tyree and Yanoulis, 1980; Steudle and Jeschke, 1983; Boyer, 1985; Dainty, 1985; Passioura, 1988; Steudle, 1993; Canny, 1995) have considered that the small area fraction and length of the cell wall bypass are reason to doubt a general dominance of this route for water transport through parenchyma tissue. Attempts to evaluate the significance of the apoplasmic route in water transport through root cortex (Ginsburg and Ginzburg, 1970; Tanton and Crowdy, 1972; Newman, 1976; Steudle and Jeschke, 1983; Bacic and Ratkovic, 1987; Radin and Matthews, 1989; Zhu and Steudle, 1991; Steudle, 1992, 1993; Zimmermann et al., 1992; Skinner and Radin, 1994; Magnani et al., 1996) and different parenchyma tissues (Tyree, 1969; Molz and Ilkenberry, 1974; Ferrier and Dainty, 1977; Steudle and Boyer, 1985) are not rare, but the results are conflicting (see Kramer and Boyer, 1995).

A good part of the discrepancies might be explained by the different degree of artificial infiltration of intercellular spaces in isolated organs and tissue and the failure of the investigators to discriminate between high- and low-resistance water transport pathways in the apoplast (cell walls, dead cells, and liquid-filled intercellular spaces). Estimations based on the specific hydraulic conductivity of Characean cell walls (Kamiya et al., 1962; Tyree, 1968; Zimmermann and Steudle, 1975) give high values for the resistance of the cell wall pathway compared with that of the protoplasmic pathway (see Newman, 1976; Passioura, 1988). Direct measurements of the hydraulic conductivity of the tangential cell wall pathway within a living parenchyma tissue are lacking.

The uniform storage parenchyma of the central core of the potato (*Solanum tuberosum* L.) tuber is a simpler matrix for volume transport than root tissues, with their specific barriers in the apoplast. Although diffusion coefficients for sugars and salts in the parenchymal apoplasts of sugar beet and storage organs of potato are not less than 30% of those in nonstirred solutions, the permeation coefficient of parenchyma slices for these low-molecular-mass osmotica (referred to as the total area) is smaller by about 2 orders of magnitude than that of a nonstirred liquid layer of equal thickness (Richter and Ehwald, 1983; Michael and Ehwald, 1996). The resistance of the living parenchyma slices to solute diffusion is large because of the small area fraction

* Corresponding author; e-mail rudolf=ehwald@rz.hu-berlin.de; fax 49–30–20–93–86–35.

Abbreviations: d, thickness of one cell wall from the protoplast to the middle lamella; D, diffusion coefficient; J_V, volume flux; l, length of the tangential cell wall pathway; L_P, hydraulic conductivity, coupling coefficient between a volume flux and an external pressure difference; L_P^{CW}, L_P of one cell wall between two cells for a volume flux in normal direction; L_P^{CWspec}, specific hydraulic conductivity of the cell wall ($\mu m^2\ s^{-1}\ MPa^{-1}$); L_P^{CWt}, L_P of the tangential cell wall pathway in the tissue slice, referred to as the whole slice area; L_{PD}, ultrafilter coefficient = coupling coefficient between an external difference in osmotic potentials and the volume flux; P, permeation coefficient of the slice for solute diffusion; PEG N, PEG with a mean molecular weight N; r, cell radius; t, slice thickness; α, apoplasmic area fraction in the slice cross-section; λ, tortuosity factor; ψ, water potential; ψ_π, osmotic potential; ψ_P, pressure potential; σ^{CW}, cell wall reflection coefficient; τ, holdup time according to Crank (1956).

of the apoplasmic pathways. Therefore, if a tissue slice is placed between two sufficiently large liquid compartments, stationary osmotic gradients can be maintained for long periods. In the present paper we report on a determination of the specific hydraulic conductivity of the parenchyma cell walls in osmotic experiments with the cell wall frame of denatured tissue slices. Furthermore, we investigated water transport through living parenchyma slices and distinguished water fluxes through protoplasts, cell walls (tangential route), and extracellular liquid spaces on the basis of the different ultrafilter properties of these pathways.

THEORY

In a denatured parenchyma slice the cell lumen has a negligible hydraulic resistance and the high-resistance pathway of the tangential cell wall route is not significant (Fig. 1). The determination of the hydraulic conductivity of the parenchyma cell wall is based on the finding that in a denatured parenchyma slice, cell walls can be treated as ultrafilter membranes with a sharp exclusion limit for polymers and a high-reflection coefficient for excluded osmotica (Carpita et al., 1979; Woehlecke and Ehwald, 1995). A stationary volume flux through the denatured slice is created by the osmotic potential difference if (a) a constant concentration difference of the polymer osmoticum is maintained between two liquid compartments separated by a denatured tissue slice, (b) the polymer osmoticum has a cell wall reflection coefficient significantly larger than 0, (c) the compartments are kept at equal pressure, and (d) the establishment of water potential gradients within the tissue has been finished.

Such osmotically driven stationary water flux should not be influenced by continuous intercellular channels (liquid-filled intercellular spaces), because the reflection coefficient of these channels is 0 even for polymer osmotica. Because of the possible occurrence of discontinuous intercellular channels the osmotically driven flux through the denatured tissue might be increased by parallel low-resistance pathways longer than the mean cell diameter. Because the small intercellular volume in the parenchyma slices consists of interconnected, continuous, and symmetric intercellular spaces, we avoided this difficulty and treated the crossed cells as resistances in a series. Therefore, the hydraulic conductivity of one separating wall between two cells is obtained by multiplying the ultrafilter coefficient of the denatured slice for a suitable osmoticum (σ^{CW} close to 1) with the number of crossed cell walls.

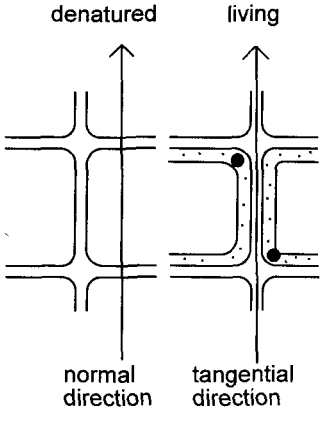

Figure 1. Cell wall pathways through denatured slices (flux in normal direction strongly dominating) and living tissue (flux through cell walls circumventing the protoplasts only possible by the tangential route).

In the complex living parenchyma tissue there are several pathways for water transport, and these are known to have different specific hydraulic conductivities and ultrafilter properties. It makes sense, therefore, to apply the possible external driving forces (osmotic and hydrostatic) separately and to compare the results. After reaching the steady state (at which influx through one face of the slice equals efflux through the other face), phenomenological coupling coefficients (L_{PD} and L_P) can be obtained from the measured flux and driving force. A flat slice can be treated as a composite membrane (compare Katchalski and Kedem, 1962; Kedem and Katchalski, 1963; Steudle, 1993), considering three parallel hydraulic pathways (Fig. 2): (a) the protoplasmic or cell-to-cell pathway (Steudle and Jeschke, 1983) combining the two possible routes from cell to cell through membranes or plasmodesmata, (b) the bypass around protoplasts through cell walls, and (c) the bypass around cells through liquid-containing intercellular spaces and other continuous extracellular channels. Because the occurrence of discontinuous intercellular channels in the living slices is not obvious, a serial arrangement of an intercellular pathway with the others is not considered.

The cell wall is a nearly perfect ultrafilter membrane for colloidal osmotica, allowing for permanent cytorrhysis in hypertonic solutions of PEGs with a molecular size above the limiting pore size (Carpita et al., 1979; Carpita, 1982). The large difference in the limiting porosity of biomembranes and cell walls enables one to apply osmotic driving forces for a volume flux through the tissue, which, in contrast to an external pressure gradient, are efficient for only one or two of the three pathways (Fig. 2).

A stationary osmotic gradient of a low-molecular-mass solute with a σ^{CW} close to 0 and membrane reflection coefficient close to 1 can only induce a volume flux through the protoplasmic pathway. A common driving force for both the pathway from cell to cell and the cell wall bypass can be created by an asymmetrically applied polymer osmoticum. If the latter is excluded from the cell wall, a concentration gradient may be established in liquid-filled intercellular spaces only, and the resulting gradient of matric potential in the cell walls (negative pressure of the liquid within intermicellar spaces) is equivalent to the water potential gradient along the protoplasmic pathway.

If stationary gradients of matric and osmotic potential along the tangential cell wall pathway are equal in magnitude and opposite in direction, no water transport through protoplasts is possible and the volume flow is restricted to the cell walls. An external pressure gradient is a common driving force for all parallel pathways.

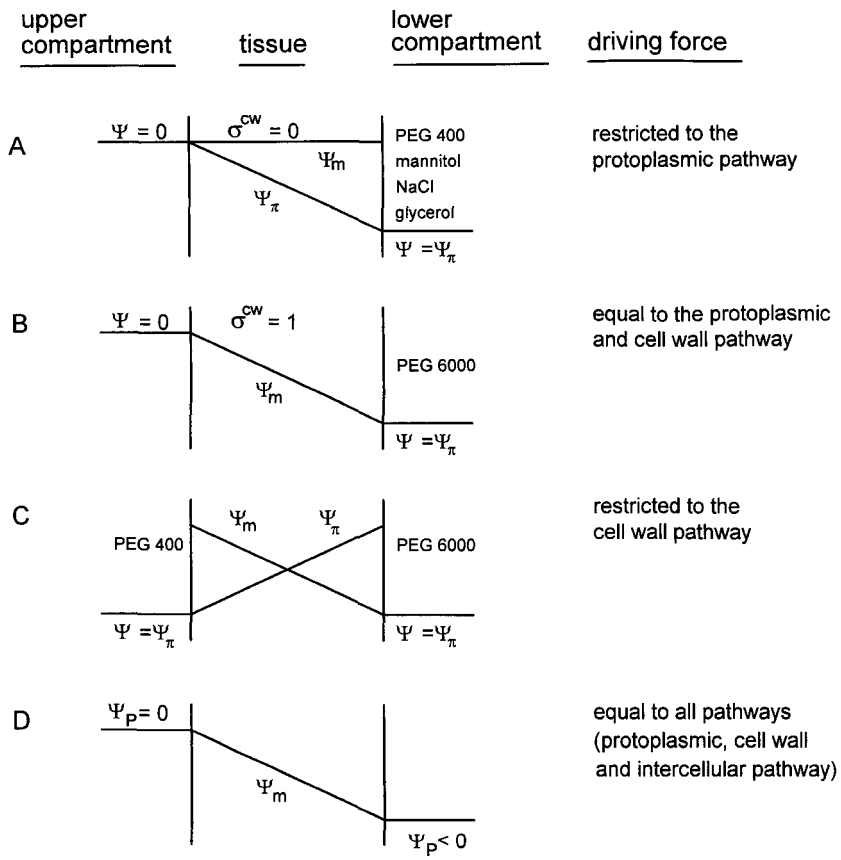

Figure 2. Action of a different osmotica and a pressure difference on the pathways involved in water transport through living tissue slices. The tissue slices are inserted like a membrane separating an upper from a lower liquid compartment (compare Fig. 3). A–C, Upper and lower compartments with different osmotica at equal hydrostatic pressure; D, application of subatmospheric pressure to the lower compartment in the absence of an osmotic potential difference. Shown gradients of components of water potential (ψ) in the tissue refer to the cell wall phase. ψ_m, Matric potential.

MATERIALS AND METHODS

Volume Changes in Denatured Parenchyma Slices

Tissue slices (3 mm thick, 12.5 mm in diameter) of potato (*Solanum tuberosum* L.) tuber were denatured and fixed in 96% ethanol and extensively washed with tap water and distilled water before starting the experiments. Subsequent volume reduction during incubation of the slices in solutions containing PEG of different molecular masses was determined gravimetrically. Before wet weight determination, the samples (10 slices) were separated from the solution by a sieve and blotted onto filter paper. Dry weight (105°C, 24 h) was determined in parallel samples. The molecular size of different commercial PEGs was estimated by a calibrated Superdex 200 H column (approximately 10,000 theoretical plates). For PEG 4,000, 6,000, and 10,000 (Serva, Heidelberg, Germany), narrow pseudomonodisperse peaks were obtained. Size dispersity of more than 90% of the polymers was found to be within the resolution limit of the column (approximately 0.2 nm in terms of Stokes' diameter).

Osmotically Driven J_Vs through Living Slices

Living tissue slices were placed between liquid compartments in polyethylene tubes (Fig. 3). The tubes were put into 20-mL glass scintillation vials as previously described (Richter and Ehwald, 1984). Slices were 4 mm thick unless otherwise noted. All experimental solutions contained 0.1 mM $CaCl_2$ and 0.1 g/L penicillin V (basic solution). A tight seal between the tube and the tissue slice was obtained in a manner similar to that described by Michael and Ehwald (1996). Tissue cylinders 12.5 mm in diameter were prepared from the central core of the tuber using a sharpened cork borer and sliced with a hand microtome and a razor blade. The slices were incubated in a shaking solution of 17.5% (w/w) PEG 6000 (ψ_π approximately −0.4 MPa). This solution was exchanged twice during an incubation period of 60 min. This pretreatment reduced (slightly) tissue volume and facilitated the introduction of the well-fitting tissue into the tube without damage. Slices were blotted onto filter paper and the border was covered with a small amount of highly viscous coconut fat (Union Deutsche Lebensmittelwerke, Hamburg, Germany). After careful fitting into the polypropylene tube, both compartments (Fig. 3) were filled with at least 2 mL of a solution of the respective osmoticum (ψ_π approximately −0.28 MPa) and shaken for 3 h. During this time slices absorbed water and the tissue was pressed to the walls of the polyethylene tube.

Different osmotic driving forces for water flux through the slices according to Figure 2 were then applied by replacing the solution in the upper compartment with a solution without osmoticum (ψ close to 0) or an isotonic solution of another osmoticum. The height difference between the liquid surfaces in the two compartments was less than 3 mm (pressure gradients less than 30 Pa). During incubation periods the vessels with the tissue slices were placed in a closed chamber to prevent evaporation and

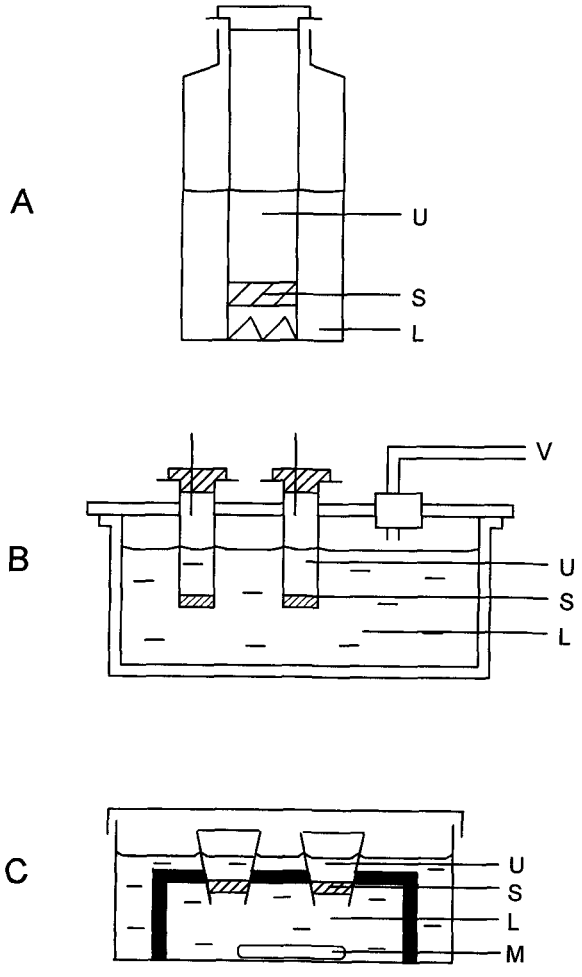

Figure 3. Variants of the two-compartment system for measurement of stationary volume and diffusion fluxes through living and denatured parenchyma. In all variants slices (usually with a diameter of 12.5 mm and a thickness of 4 mm) were fitted into polyethylene tubes. The slices (S) in the tubes were then covered by liquid (upper compartment, U) and the tubes set into vessels with liquid (lower compartment, L). In variant A (used for investigation of osmotically driven volume fluxes and for diffusion experiments), tubes were placed into 20-mL glass vials and covered (not tightly) by polyethylene lids. Liquid levels in U and L were equal. For facilitating convectional exchange, tubes were slotted below the slice position. Vessels with tubes were fixed in a closed chamber, which was shaken at room' temperature. In variant B (used for measuring pressure-driven volume fluxes through living slices), the covering plate of a suction vessel was connected with a low-pressure chamber and vacuum pump (V). The chamber was filled with tap water. Polyethylene tubes were filled above the slices (S) with 3 mL of tap water (U) and plugged into the holes of the covering plate, whereby the lower faces of slices were in contact with the water in the suction vessel (L). Pressure exchange of the water in U with the atmosphere was enabled by a cannula in the tube stopper. In variant C (used for measuring volume fluxes through denatured slices), a stand with a supporting plate for slightly conical tubes containing slices (S) was set into a chamber with a solution of PEG 6000 (L), which was stirred by a magnetic stirrer (M). Solutions in U were equal to those in L (control experiment) or did not contain PEG 6000 (volume-flow experiment).

shaken with a frequency of about 2 s^{-1}. For gravimetric determination of volume changes in the upper compartments, the tubes with the tissue were taken out of the vessels and adhering liquid from the lower compartment was sucked off carefully by means of a capillary connected to a vacuum pump. The first weighing was carried out 3 h after setting up the osmotic gradient. Osmotically driven water fluxes through the tissue were nearly constant for at least 2 d. Ultrafilter coefficients ($L_{PD} = J_V/\Delta\psi_\pi$) were determined from the change in weight, slice area, time interval, and difference in osmotic potential. Osmotic potentials of applied solutions with polymer and low-molecular-mass solutes were determined using a vapor pressure osmometer (Knauer, Berlin, Germany).

J_Vs through Living Slices Driven by a Stationary External Pressure Gradient

The tubes with the living tissue slices were tightly fitted into a solid plate, which was covering a cylindrical desiccator vessel (Fig. 3). The tissue slices at the lower end of the tubes dipped into a large water reservoir within the vessel. The latter was kept under subatmospheric pressure (0.06 MPa), whereas the upper compartments (also containing water) were connected with the atmosphere by thin cannulas. Fluxes were measured gravimetrically as described above.

J_Vs through Denatured Tissue Cylinders

Tissue cylinders (diameter 12.5 mm, thickness 4 mm) were prepared and denatured in 96% ethanol as described above. The slices were rehydrated by washing overnight in a solution of 0.1 mM $CaCl_2$ and 1.5 mM NaN_3, carefully blotted with cotton tissue, and allowed to evaporate 8% of the tissue water. The slightly shrunken slices were carefully placed into polyethylene tubes by means of a fitting cylinder (Fig. 3). These tubes were conical (angle between tube wall and tube axis 2.5°). At the area of contact with the denatured tissue, the inner tube wall was covered by a thin layer of stopcock grease. For each experiment, 16 parallel tubes with tissue slices were inserted into a solid supporting plate within a stirred chamber (Fig. 3). The stirred vessel (lower compartment) contained a solution of 1.5 mM NaN_3, 0.1 mM $CaCl_2$, and PEG 6000 as osmoticum (3.3 g L^{-1}, $\psi_\pi = -1.34$ kPa). The tube lumen above the slice (upper compartment) was filled with either about 1 mL of the same solution (control) or a solution of the mentioned salts without PEG. Differences in height between the liquid level in the lower and upper compartments were carefully avoided. Weighing of the tubes (with the upper compartment and loosely fitting lid) was carried out as described above. Control tubes with equal concentrations of PEG 6000 in both compartments did not show a significant weight change. Ultrafilter coefficients of the denatured tissue were calculated from the weight change between the 6th and 20th h of incubation (about 30 mg).

Kinetics of Diffusion of α-Methylglucoside through Living Tissue

Glass vials with the two-compartment system (Fig. 3) were applied in such a way that the lower compartment contained 50 mM α-methylglucoside and 50 mM mannitol (4 mL) and the upper compartment contained 100 mM mannitol (0.25 mL). The liquid in the upper compartment was exchanged periodically and the α-methylglucoside concentration was determined by a colorimetric method based on glucoseoxidase, peroxidase, and o-dianisidine (Ehwald and Göring, 1972) after demethylation of the glucoside with α-glucosidase.

Effect of a Cell Wall Matric Potential Gradient on Permeation of [U-^{14}C]Mannitol through the Living Tissue

Living parenchyma slices (4 mm in thickness) were fitted in the shaken two-compartment system as described above (Fig. 3). Solutions in both compartments contained 10 mM Glc and 10 mM mannitol. In all variants the solution in the lower compartment (2 mL) contained PEG 400 at a concentration of 4.2% (w/w) (0.28 MPa). In the upper compartment the solution (1 mL) contained either 4.2% PEG 400 (control variant) or 15.0% (isotonic) PEG 6000 to create a selective driving force for the volume flux through cell walls. After 3 h of preincubation, the solution in the upper compartment was exchanged for a solution of equal composition containing [U-^{14}C]mannitol (25 kBq mL^{-1}). The tubes were transferred to new vessels with unlabeled solution of the same composition after another 4 h (when a steady-state gradient was reached). For determination of the mannitol flux, radioactivity in the lower compartment was measured by a liquid-scintillation counter after an incubation period of 17 h.

Infiltration and Determination of the Volume Fraction of Air-Filled Intercellular Spaces in the Tissue

The slices were infiltrated with the respective solution (PEG solution, tap water) by repeated application of a vacuum (three 5-min applications). The volume of infiltrated (formerly gas-filled) intercellular spaces was determined by means of the tissue-density change (determination of the isopycnic Suc concentrations before and after infiltration; see Richter and Ehwald, 1983).

Pressure-Probe Experiments

Pressure-relaxation experiments were carried out in the usual way (Hüsken et al., 1978; Steudle, 1993) with a cell pressure probe using capillaries with a tip width of 5 to 8 μm, whereby the investigated tissue (a tissue slice about 4 mm in thickness) was kept in contact with tap water and air at room temperature. Reported values of turgor pressure, volume elasticity modulus, and half-time of pressure relaxation refer to experiments with cells showing stable baseline turgor pressure. After inserting the capillary into the tissue, the first stable recording (the first inserted cell) was used for fixing the meniscus position outside the tissue. Pressure-relaxation experiments were then carried out after successful insertion of the capillary into a following cell, by either increasing (+) or decreasing (−) the volume of liquid. Measurements with three repeated (+) and (−) relaxation curves were accepted.

RESULTS

Osmotically Driven J_Vs through Cell Walls of Denatured Slices

Denatured tissue slices shrink transiently in PEG solutions with molecular masses of 1000, 1500, and 2000 D, showing a fast "water phase" and a slow "solute phase," whereas shrinkage was permanent in solutions of PEG with a molecular mass of 4000 D and higher (Fig. 4). At steady state or equilibrium, when the volume of the compressed tissue slice has reached its minimum or final volume ($J_V = 0$), a cohesion tension in the cells of the deformed tissue ($-\Delta\psi_P$) has to be assumed to compensate the osmotic driving force. Tissue shrinking in solutions of PEG 6000 was reversible. Slices regained their original volume by reswelling in the basic mineral solution (not shown).

In the case of PEGs with a molecular mass above 4 kD the solute phase (reswelling by entrance of PEG solution into the lumina of denatured cells) was not detectable in a period that was more than 20 times longer than the half-time of the shrinkage (water phase). Together with the independence of the shrinkage rate from molecular size, this proves that the σ^{CW} for the three investigated larger PEGs is close to 1. Figure 4 also shows that the σ^{CW} of PEG 2000 and PEG 1500 are significantly less than 1 and that that of PEG 400 is close to 0.

Because the intercellular spaces are very small, outer cell layers cannot shrink strongly without affecting the volume of the inner cells. Indeed, shrinkage of the slices in diameter (not shown) and the decrease in fresh weight showed similar time curves. The evaluation of shrinkage kinetics for determination of cell wall permeability is difficult for this and various other reasons. Therefore, we determined

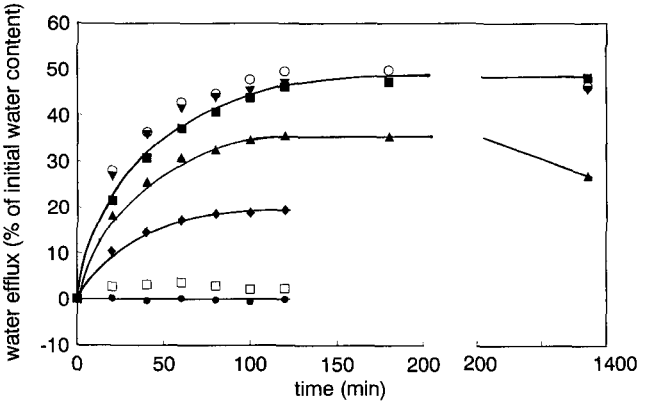

Figure 4. Shrinkage of denatured tissue slices induced in isotonic PEG solutions ($\psi_\pi = -65$ kPa) of different molecular masses (slice thickness 3 mm, diameter 12.5 mm). ●, PEG 400; □, PEG 1000; ◆, PEG 1500; ▲, PEG 2000; ○, PEG 4000; ▼, PEG 6000; and ■, PEG 10,000.

the hydraulic conductivity of cell walls with the two-compartment system by measuring stationary J_Vs through the denatured tissue slices (Fig. 3). At small stationary osmotic driving forces ($\Delta\psi_\pi$ less than 2 kPa), the slice volume remained constant during the measuring time. A refractometer ensured that within the investigation period (20 h) the PEG concentration gradient was not decreased (no measurable change in the upper compartment). Because σ^{CW} was close to 1, the hydraulic conductivity of one wall between two cells, $L_P{}^{CW}$, was obtained from L_{PD} of the denatured slice by counting the number (n) of crossed cell layers and treating the (n + 1) walls as resistances in a series (Table IA). The $L_P{}^{CW}$ of a cell wall between two protoplasts was large (approximately 40 $\mu m\ s^{-1}\ MPa^{-1}$) compared with that of typical biomembrane values measured with the cell pressure probe, including that of potato parenchyma cells (approximately 0.5 $\mu m\ s^{-1}\ MPa^{-1}$; see below).

Contribution of the Cell Wall Bypass to the L_P of Living Tissue Slices

To determine the $L_P{}^{CWspec}$, the mean thickness of one wall separating two protoplasts must be known. The thickness of the dehydrated cell wall measured in ultrathin slices by electron microscopy is smaller than that of the swollen wall in vivo. To get a realistic estimate of the area fraction of the cell walls between protoplasts, we determined the apoplasmic area fraction in the cross-section of the living tissue that is available for diffusion of α-methylglucoside (compare Richter and Ehwald, 1983; Michael and Ehwald, 1996). The time course of diffusion of α-methylglucoside through a 3-mm-thick living parenchyma slice is shown in Figure 5.

Because this nonelectrolyte is taken up very slowly by the protoplasts of plant cells (Fleischer and Ehwald, 1995), its diffusion kinetics are determined by the available apoplasmic area fraction in the cross-section of the living tissue (α), the length of the tangential cell wall pathway (l), and the diffusion coefficient in the apoplast (D). The diffusion coefficient, D (which is independent of α), was obtained from the pathway length, l, and the "holdup time," τ (Crank, 1956), which is the intersection of the time scale with the straight line obtained for steady-state permeation (Fig. 5). α was found to be 0.017 (Table IB). On the basis of the nearly isodiametric (polyedric) shape of the cells and the small volume of intercellular spaces (see below), it is possible to calculate a mean estimate for the thickness of one cell wall, i.e. the distance from the plasmalemma to the middle lamella (see "Appendix"). In this way, a mean thickness ($2d$) of the hydrated wall between two cells of approximately 1.2 μm is obtained (Table IB).

Assuming an isotropic resistance to water transport, $L_P{}^{CWspec}$ is available from $L_P{}^{CW}$ and the thickness estimate of the cell wall (Table IC). If calculated from these estimates, the hydraulic conductivity of the tangential cell wall pathway referred to the whole slice area, $L_P{}^{CWt}$, is very small (compare the value shown in Table IC with L_P or L_{PD} of living slices given in Tables II and IIIA).

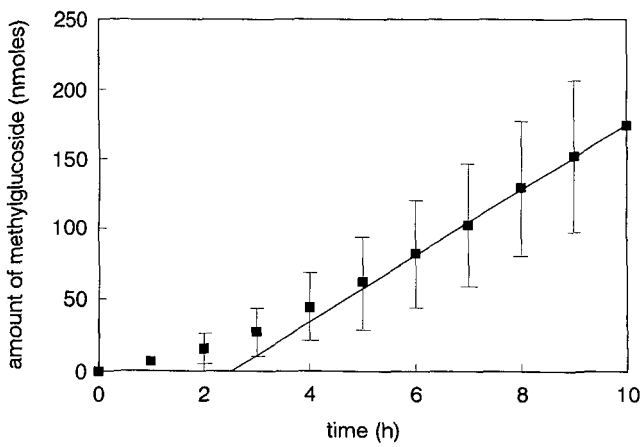

Figure 5. Time course of diffusion of α-methylglucoside through 3-mm-thick living parenchyma slices (cross-sectional area of 1.23 cm^2). Mean values of 10 parallel experiments with confidence intervals (P = 95%). The slope of the straight line represents the stationary flux into the lower compartment and corresponds to a permeation coefficient of the tissue slice, P_t. The intercept of this line with the time axis is the holdup time, τ, corresponding to an apoplasmic diffusion coefficient D (for values, see Table IB).

Coupling Coefficients of Living Slices for Pressure-Driven and Osmotically Driven J_Vs

In living potato tissue slices the volume of intercellular spaces is small, but these spaces are interconnected and

Table IA. *L_P of the cell wall in the normal direction ($L_P{}^{CW}$) obtained from water flow through denatured 4-mm-thick parenchyma slices*

Values are means with confidence intervals (P = 95%, n = 12).

L_{PD} of denatured slices ($\mu m\ s^{-1}\ MPa^{-1}$)	
Experiment I	−1.6 ± 0.6
Experiment II	−2.3 ± 0.9
Mean value	1.95
$L_P{}^{CW} \approx -L_{PD}{}^{CW}$ referred to one separating wall	41 $\mu m\ s^{-1}\ MPa^{-1}$

Table IB. *Parameters of diffusion of α-methyl-glucopyranoside through living slices (thickness, 3 mm) and estimation of the cell wall thickness*

Permeation coefficient[a] (P_t)	1.0 nm s^{-1}
Holdup time[b] (τ)	9.63 10^3 s
Length of cell wall pathway (l)	3.4 mm
Apoplasmic diffusion coefficient (D)	2.0 10^{-10} $m^2\ s^{-1}$
Tortuosity factor[c] (λ)	1.13
Effective area fraction, α = D/(P × 1) (α)	0.017
Cell radius[d] (r)	100 μm
Thickness of wall between two cells ($2d$) (see "Appendix")	1.2 μm

[a] Obtained from the stationary flux (Fig. 5) through the slice area. [b] Obtained from time curve of diffusion (Fig. 5). [c] Determined by a curvimeter in microphotos. [d] Determined by counting the cell layers of slices.

Table IC. *Specific L_P of parenchyma cell wall and derived values*

L_P^{CWspec} (= $L_P^{CW} \times 2d$)	49.1 $\mu m^2\ s^{-1}\ MPa^{-1}$
L_P^{CW}	
In a 4-mm slice ($L_P^{CWt4mm} = L_P^{CWspec} \times \alpha/[4\ mm\ \lambda]$)	0.18 $nm\ s^{-1}\ MPa^{-1}$
Of one cell layer ($L_P^{CWt} = L_P^{CWspec} \times \alpha/[2r\ \lambda]$)	3.7 $nm\ s^{-1}\ MPa^{-1}$

partly (near the cut surface) infiltrated with liquid. There can be no doubt regarding the presence of continuous liquid-filled intercellular channels in the cut region near the tube wall, because this region was translucent in contrast to the major part of the slice. To check the significance of the intercellular pathway for L_P, we determined the volume fraction of intercellular air in the tissue and measured pressure-driven fluxes through noninfiltrated and infiltrated parenchyma slices (Table II). L_P increased dramatically (about eight times) by infiltration, although the density measurements revealed replacement of a rather small air volume (0.8% of tissue volume) by water. Using slices of different diameter, it was found that the pressure-driven J_Vs were proportional to the slice diameter in nontreated slices and proportional to the slice area in vacuum-infiltrated slices (results not shown). Although the infiltrated volume at the slice border is a minor fraction of the whole intercellular space, which is about 1% of the tissue volume, the L_P of the noninfiltrated slices was higher than $-L_{PD}$ by about 1 order of magnitude.

The L_P of infiltrated slices (Table II) was low enough to ensure that the small pressure gradients (less than 30 Pa) developing in osmotic experiments did not have significant influence on measured L_{PD}. In a parenchyma slice the intercellular liquid channels are not separated from the external medium by a microporous membrane. Therefore, differences in external osmotic potential (independent of the size of the osmoticum) should not induce volume flow through this extracellular pathway. The L_{PD} of living slices, in contrast to L_P, was not dependent on infiltration and diameter (Table II).

It follows from results shown in Figure 4 that the contribution of the cell wall bypass to L_{PD} of the living slices approximates the maximum value if PEG with a molecular mass of more than 4 kD is used as osmoticum, whereas no significant contribution of this pathway can be expected if L_{PD} is measured by means of an osmoticum with low molecular mass. However, L_{PD} values obtained with PEG 400, mannitol, and NaCl were not significantly different from those obtained with PEG 6000 (Table IIIA). L_{PD} was not altered by increasing the ion strength. The value obtained with glycerol (reflection coefficient of cell membranes less than 1) was the smallest (difference not statistically significant). The results shown in Table IIIA demonstrate that the cell wall bypass is of minor importance for water transport through the investigated tissue (compare Fig. 2).

In arrangement C, shown in Figure 2, the external osmotic gradients should allow for an apoplasmic volume flux without protoplasmic water transport. In this experimental arrangement, fluxes were smaller than the accuracy of the gravimetric method (data not shown). Asymmetric application of PEG had no significant influence on the permeation of mannitol, which can be assumed to take place in the apoplast. The water flux induced by 15% PEG 6000 (−0.28 MPa, 4-mm slice) amounted to about 5 $nm\ s^{-1}$, i.e. about 10 times the permeation coefficient of the slice for mannitol. Therefore, even a small contribution of the apoplasmic pathway to water transport should cause a significant solvent drag effect, but no such effect was observed. Obviously, the volume flux in the tangential cell wall pathway was smaller than the common confidence interval (approximately 0.08 $nm\ s^{-1}$) of permeability coefficients of mannitol measured in the absence and presence of the PEG concentration gradient (Table IIIB). This is coincident with a contribution of the cell wall pathway to L_{PD} of less than $-0.25\ nm\ s^{-1}\ MPa^{-1}$, or less than 2% of the overall value.

Table II. *Effect of vacuum infiltration on coefficients coupling volume flux through 4-mm-thick slices with differences of hydrostatic (L_P) and osmotic pressure (L_{PD})*

Values are means ± SD.

Parameter	Parallels	Slice Diameter	Nontreated	Vacuum Infiltrated
		mm	*kg L^{-1}*	
Mean density of isopycnic Suc solution	10	12.5	1.0668	1.0748
				%
Infiltrated volume fraction				0.8
			$\mu m\ s^{-1}\ MPa^{-1}$	
L_P[a]	6	12.5	0.335 ± 0.214	2.701 ± 0.794
			$nm\ s^{-1}\ MPa^{-1}$	
$-L_{PD}$[b]	6	12.5	20.7 ± 4.8	19.2 ± 3.2
	7	9.8	18.0 ± 2.8	
	8	12.5	18.2 ± 4.9	
	10	16.0	21.5 ± 4.7	

[a] $\Delta\psi_P = 0.04$ MPa, $\Delta\psi_\pi = 0$. [b] $\Delta\psi_\pi = -0.28$ MPa, $\Delta\psi_P = 0$, osmoticum PEG 6000.

Table IIIA. *Ultrafilter coefficients (L_{PD}) obtained from stationary J_Vs driven by gradients of different osmotica ($\Delta\psi_\pi$ = −0.28 MPa) through 4-mm-thick parenchyma slices*

Values are means with confidence intervals in parentheses (P = 95%, n = 12).

Experiment	Osmoticum	$-L_{PD}$
		nm s^{-1} MPa^{-1}
1	PEG 6000	17.1 (13.5–20.7)
	PEG 400	16.9 (13.6–20.2)
	PEG 6000[a]	15.3 (12.5–18.1)
	PEG 400[a]	15.9 (14.0–17.8)
2	PEG 6000	16.3 (14.7–17.9)
	PEG 400	15.1 (13.1–17.1)
	Mannitol	14.3 (12.9–15.7)
	NaCl	16.0 (13.3–18.7)
	Glycerol	12.0 (8.0–16.0)

[a] 10 mM NaCl present in both compartments.

Comparison of L_{PD}s of the Slices with the L_P of Single Cells

In experiments with slices of different thickness, it was found that the product of L_{PD} and slice thickness (t) was not significantly different in the variants (Table IVA). Because the different cell layers can be regarded as resistances in series, we compared L_{PD} of tissue slices with L_P of single parenchyma cells obtained by means of the cell pressure probe from pressure-relaxation kinetics. Values of cellular L_P were nearly twice the $-L_{PD}$ value that was calculated for one cell layer (compare Tables IVA and IVB).

DISCUSSION

Specific L_P of Parenchyma Cell Walls

With regard to the polymer size limits for permeation through the cell walls, the investigated parenchyma is similar to other plant materials (compare Carpita et al., 1979; Carpita, 1982; Woehlecke and Ehwald 1995). As shown previously (Ehwald et al., 1992), the denaturing treatment of the tissue with ethanol has no irreversible influence on the limiting cell wall porosity. The critical Stokes' diameter (5.2 nm) of dextran molecules for preventing diffusion through the cell walls of the denatured potato storage parenchyma (Woehlecke and Ehwald, 1995) is slightly larger than the chromatographically determined Stokes' diameter of PEG 4000 (4.8 nm), which seems to be near the critical value for reaching the maximum L_{PD} (Fig. 4).

The L_P of a cell wall between two cells (estimated thickness, 1.2 μm) for a flux in the normal direction is about 40 μm s^{-1} MPa^{-1} (Table IC). This is little more than 5% of the value obtained by Poiseuille's law for a 1.2-μm-long cylindric capillary with a diameter of 5 nm and the viscosity of water at 20°C. It has to be kept in mind that both the size limit of permeation and L_P^{CW} are determined by the largest hydraulic channels through the wall, which represent only a fraction of the cell wall area. The value we determined for L_P^{CWspec} (49 μm^2 s^{-1} MPa^{-1}) is in the same range of magnitude as those determined for Characean cell walls (Kamiya et al., 1962; Tyree, 1968; Zimmermann and Steudle, 1975).

Zhu and Steudle (1991) compared half-times of turgor pressure relaxation after hydrostatic and osmotic changes in different layers of the maize primary root (using KCl and PEG 6000 as osmotica). Applying a model based on parallel fluxes through only radial cell walls and protoplasts they calculated L_P^{CWspec}. The resulting values were much higher (up to 6100 μm^2 s^{-1} MPa^{-1}) than the Characean values and our estimate. However, the model of Zhu and Steudle (1991) implies presuppositions that may be doubted, e.g. that after application of an external osmoticum "within the tissue, the driving forces are matric or hydrostatic in nature rather than osmotic," the apoplasmic bypass is represented by the radial cell wall pathway, and pressure-relaxation kinetics in inserted cells of inner cortex layers are independent of the hydraulic and diffusive channel (killed cells) created by driving the capillary through the cortex.

Significance of the Cell Wall Bypass for Tissue Hydraulics

The measured value for the cell wall L_P (Table IC) is 2 orders of magnitude greater than membrane L_P values determined for the single cells in the same tissue (Table IVB). The thickness of one cell-separating wall is about 120 times the biomembrane thickness. The tangential cell wall path, however, if calculated for one cell layer, is longer than the membrane thickness by a factor of 3×10^4. Considering further the small area fraction of the tangential cell walls in the tissue cross-section (<1.7%), the estimated L_P^{CWt} (0.18 nm s^{-1} MPa^{-1}; Table IC) is small in compari-

Table IIIB. *Influence of a matric potential gradient in the cell wall on mannitol flux through 4-mm-thick parenchyma slices*

Values are means with confidence intervals in parentheses (P = 95%, n = 12), obtained from the steady-state flux of ^{14}C into the lower compartment (5–21 h after labeling the upper compartment). Both compartments contained nonlabeled mannitol (10 mM), and both compartments in variant A and the lower compartment in variant B contained PEG 400 in a concentration that was isotonic to the solution of PEG 6000.

	Concentration of PEG 6000 in the Upper Compartment	Matric Potential Gradient in Cell Walls	Permeation Coefficient of [^{14}C]Mannitol
	% (w/w)	*MPa*	*nm s^{-1}*
A	0	0	0.53 (0.49–0.57)
B	15	−0.28	0.56 (0.49–0.63)

Table IVA. *Ultrafilter coefficients (L_{PD}) and derived values obtained with tissue slices of different thickness*

Values are means with confidence intervals (P = 95%, n = 15), obtained from stationary volume fluxes driven by concentration differences of PEG 6000 ($\Delta\psi_\pi$ = 0.28 MPa).

t (mm)	3	4	6
No. of crossed cell layers (n)	15	20	30
		nm s^{-1} MPa^{-1}	
− L_{PD} of the tissue slice	18.0 ± 2.7	14.5 ± 3.3	10.8 ± 1.9
		μm^2 s^{-1} MPa^{-1}	
− L_{PD} × t (specific ultrafilter coefficient)	54 ± 8	58 ± 13	64.6 ± 11
		μm s^{-1} MPa^{-1}	
− L_{PD} × $2n$ (ultrafilter coefficient of one layer of living cells)	0.54	0.58	0.65

son with the L_{PD} of the whole living tissue slice (approximately 15 nm s^{-1} MPa^{-1}; Tables IIIA and IVA).

Inefficiency of the cell wall bypass was shown directly by experiments with the living parenchyma. The nearly equal fluxes driven by isotonic concentration differences of osmotica with undercritical and overcritical sizes (σ^{CW} close to 0 or 1) and the absence of any measurable solvent drag effect induced by 15% PEG 6000 (Table IIIA) prove that the contribution of the protoplasmic hydraulic pathway to the whole water flux is much greater than that of the bypass through walls.

The hydraulic permeability of the cell wall bypass was too small to be experimentally quantified by the difference between L_{PD} values of living slices for colloidal and low-molecular-mass osmotica. Results obtained by the solvent drag experiments, which were more accurate (Table IIIB), show that the tangential cell wall pathway does not contribute to L_{PD} of the whole tissue by more than 0.3 nm s^{-1} MPa^{-1}. This value, an upper limit, is slightly larger than the estimate of the L_P of the tangential cell wall pathway based on the assumption of a hydraulically isotropic cell wall material (Table IC).

We cannot exclude a significant anisotropy of the cell wall with respect to its L_P, but a possible preference of the tangential direction would not be large enough to render the cell wall bypass significant. Control of tissue L_{PD} by the hydraulic properties of protoplasts seems to be confirmed by its comparison with pressure-probe values (Tables IVA and IVB).

Ginsburg and Ginzburg (1970) and Schambil and Woermann (1989) used axial perfusion of maize root sleeves (root segments from which the central cylinder was removed) to measure osmotically driven volume fluxes through the cortex. Without regard to the polarity and higher complexity of the investigated extrastelar root tissue, the experimental arrangement was the same as that used here for measuring the L_{PD} of living potato slices (stationary volume fluxes measured between agitated liquid compartments in the absence of external pressure differences, concentration differences kept constant, external unstirred layers nonsignificant). Authors of both cited papers found that the L_{PD} of the sleeve tissues for PEG 2000 was not significantly different from the L_{PD} for sugars (Suc and raffinose). We found (W. Michael and R. Ehwald, unpublished data) that PEG 2000, in contrast to the sugars, induced significant reversible shrinkage of the denatured maize root cortex. Therefore, considering the arguments given above, nearly equal L_{PD} values of sleeves for PEG 2000 and sugars suggest the dominance of the protoplasmic pathway over the cell wall bypass through the root cortex.

Signficance of Liquid-Filled Intercellular Spaces and Other Nonselective Channels for Tissue Hydraulics

It may be inferred from the data shown in Table II that a very small additional volume fraction of nonselective channels (0.8% of the whole-tissue volume) increased the hydraulic permeability of the living slices in the two-compartment system by a factor of 8 but did not have any significant effect on the ultrafilter coefficient, L_{PD}. This demonstrates that the infiltrated volume is represented by continuous macroscopic channels, which are effective pathways for water only in cases of external pressure difference (see "Theory"). Even in the infiltrated case, the hydraulic permeability of the slices was too low for an effect of the small pressure differences (ΔP < 30 Pa) existing in the experimental system at measurement of L_{PD} (variant A in Fig. 3).

It may also be assumed from the data shown in Table II that in our measuring system (ΔP < 30 Pa, $\Delta\psi_\pi$ = 0.28 MPa) the product $L_P \times \Delta\psi_P$ is negligible in comparison with the product $L_{PD} \times \Delta\psi_\pi$. Table II shows that the cell wall pathway (which is characterized by a dense matrix) should be separated from possible extracellular continuous pathways through intercellular spaces in the living tissue or in the wounded region near the tube walls, which may be very efficient for pressure-driven flow, even if their relative

Table IVB. *Data obtained from pressure-relaxation experiments with cell pressure probe*

Cell radius[a]	56 μm
Osmotic potential of cell sap[a]	−0.7 MPa
Turgor pressure[b]	0.484 ± 0.027 MPa
Volume elasticity modulus[b]	5.22 ± 0.17 MPa
Half-time of pressure relaxation[b]	4.9 ± 1.6 s
Hydraulic permeability of the cell membranes	0.44 μm s^{-1} MPa^{-1}

[a] Determined on tissue level. [b] Mean values with SD.

area is very small. The often-used term "diffusivity" for L_P^{CWspec} is misleading. In remarkable contrast to the diffusion coefficients of the cell wall phase for water and low-molecular-mass solutes, which are a little smaller than those of nonstirred water (Michael and Ehwald, 1996), L_P^{CWspec} of the cell wall is at least 4 orders of magnitude smaller than that of liquid-filled intercellular channels. This follows from Poiseuille's law:

$$L_p^{spec} = \text{constant} \times w^2$$

if the effective channel width, w, in each system is considered. Therefore, liquid-filled intercellular or extracellular spaces, if present, should be the largely dominating pathways for pressure-driven water transport through a tissue, even at small volume fractions. As shown in Table II, this is true for living infiltrated parenchyma slices, which have a very small but highly permeable volume fraction of intercellular spaces. Because of the nonavoidable infiltration at the cuts and possible further artificial channels at the tube walls, the L_P values given in Table II for noninfiltrated slices are not informative to the situation in situ. The results show, impressively, that the apoplasmic water transport pathways along cell walls must be treated separately from those along liquid-filled intercellular spaces. Although this conclusion can hardly be doubted, in many papers on radial water transport through the root cortex the apoplastic pathways are not differentiated.

The apoplast of a living parenchyma tissue must be regarded as a three-phase system, consisting of the immobile polymers of the cell wall matrix, a liquid phase, and a gaseous phase. This is analogous to the situation in the soil, in which "nonsaturated flow" has gotten much attention (Jury et al., 1991). Passioura (1988) has pointed to the possibility that intercellular spaces contribute to water transport in situ. In water-saturated living roots and storage organs most of the intercellular spaces are kept free of liquid. The reason seems to be the hydrophobic nature of the intercellular cell wall surface (Wooley, 1983; Passioura, 1988). Much evidence has been found for the strong hydraulic efficiency of nonselective extracellular channels between cortex and xylem in roots, e.g. in secondarily altered regions, at positions of lateral root emergence or artificial puncturing (see Steudle et al., 1993). Although liquid filling of a considerable part of the intercellular spaces has been claimed to occur in the root cortex (Canny and Huang, 1993), there is not enough information on the amount and continuity of apoplasmic liquid outside of cell walls in nonwounded cortex and parenchyma tissues. The significance of a possible discontinuous apoplasmic water transport pathway through the intercellular spaces of the nondamaged primary root cortex remains an open question.

APPENDIX

Estimation of the Cell Wall Thickness

For estimation of the cell wall thickness, d (the distance between plasmalemma and middle lamella), from the apoplasmic area fraction, α, the tissue was assumed to consist of thin-walled polyedric cells with nearly spherical cross-sections, the mean radius (r) of which is 100 μm. d is estimated from $\alpha = 0.017$ (Tables I, A, B, and C, and II), which may be approximately set equal to the volume fraction of the cell wall with thickness d:

$$\alpha = 0.017 \approx d \times 3/r \; (d \approx 0.6\ \mu\text{m}).$$

Because the parenchyma cells are polyeders and liquid-filled intercellular spaces (minor part) are included in the value of α, the cell wall thickness, d, is slightly overestimated this way.

Received January 30, 1997; accepted July 21, 1997.

LITERATURE CITED

Anderson WP (1976) Transport in roots. *In* U Lüttge, MG Pitman, eds, Encyclopedia of Plant Physiology. Transport in Plants II, Part B: Tissues and Organs. Springer-Verlag, Berlin, pp 129–156

Bacic G, Ratkovic S (1987) NMR studies of radial exchange and distribution of water in maize roots: the relevance of modelling of exchange kinetics. J Exp Bot **38:** 1284–1297

Boyer JS (1985) Water transport. Annu Rev Plant Physiol **36:** 473–516

Canny MJ (1995) Apoplasmic water and solute movement: new rules for an old space. Annu Rev Plant Physiol Plant Mol Biol **46:** 189–214

Canny MJ, Huang CX (1993) What is in the intercellular spaces of the roots? Evidence from cryo-scanning microscope. Physiol Plant **87:** 561–568

Carpita N (1982) Limiting diameter of pores and surface structure of plant cell walls. Science **218:** 813–814

Carpita N, Sabularse D, Montezinos D, Delmer DP (1979) Determination of pore size of cell walls of living plant cells. Science **205:** 1144–1147

Crank J (1956) The Mathematics of Diffusion. Clarendon Press, Oxford, UK

Dainty J (1985) Water transport through the root. Acta Hortic **171:** 21–31

Ehwald R, Göring H (1972) Application of glucoseoxidase for microdetermination of glucose and sucrose in plant tissues (in Russian). Fiziol Rast **17:** 1105–1109

Ehwald R, Woehlecke H, Titel C (1992) Cell wall microcapsules with different porosity from suspension cultured *Chenopodium album*. Phytochemistry **31:** 3033–3038

Ferrier JM, Dainty J (1977) Water flow in *Beta vulgaris* storage tissue. Plant Physiol **60:** 662–665

Fleischer A, Ehwald R (1995) The free space of sugars in plant tissues: external film and apoplastic volume. J Exp Bot **46:** 647–654

Ginsburg H, Ginzburg BZ (1970) Radial water and solute flow in roots of *Zea mays*. J Exp Bot **21:** 580–592

Hüsken D, Steudle E, Zimmermann U (1978) Pressure probe technique for measuring water relations of cells in higher plants. Plant Physiol **61:** 158–163

Jury AW, Gardner WR, Gardner WH (1991) Soil Physics. John Wiley & Sons, New York

Kamiya N, Tazawa M, Takata T (1962) Water permeability of the cell wall in *Nitella*. Plant Cell Physiol **3:** 285–292

Katchalsky A, Kedem O (1962) Thermodynamics of flow processes in biological systems. Biophys J **2:** 53–78

Kedem O, Katchalsky A (1963) Permeability of composite membranes. Part 2. Parallel elements. Trans Far Soc **59:** 1931–1940

Kramer PJ, Boyer JS (1995) Water Relations of Plants and Soils. Academic Press, San Diego, CA, pp 186–187

Läuchli A (1976) Apoplasmic transport in tissues. *In* U Lüttge, MG Pitman, eds, Encyclopedia of Plant Physiology. Transport in Plants II, Part B: Tissues and Organs. Springer-Verlag, Berlin, pp 3–34

Magnani F, Centritto M, Grace J (1996) Measurement of apoplasmic and cell-to-cell components of root hydraulic conductance by a pressure-clamp technique. Planta **199:** 296–306

Michael W, Ehwald R (1996) Exchange diffusion of alkali ions through the apoplast of potato (*Solanum tuberosum* L.) storage parenchyma. Plant Cell Environ **19:** 243–246

Molz FJ, Ilkenberry E (1974) Water transport through plant cells: theoretical development. Soil Sci Soc Am Proc **38:** 699–704

Myers GMP (1951) The water permeability of unplasmolysed tissues. J Exp Bot **2:** 129–144

Newman EI (1976) Water movement through root systems. Philos Trans R Soc Lond B **273:** 463–478

Passioura JB (1988) Water transport in and to roots. Annu Rev Plant Physiol Plant Mol Biol **39:** 245–265

Pitman MG (1977) Ion transport into the xylem. Annu Rev Plant Physiol **28:** 71–88

Radin J, Matthews M (1989) Water transport properties of cortical cells in roots of nitrogen- and phosphorus-deficient cotton seedlings. Plant Physiol **89:** 264–268

Richter E, Ehwald R (1983) Apoplastic mobility of sucrose in storage parenchyma of sugar beet. Physiol Plant **58:** 263–268

Schambil F, Woermann D (1989) Radial transport of water across cortical sleeves of excised roots of *Zea mays* L. Planta **178:** 488–494

Skinner RH, Radin JW (1994) The effect of phosphorus nutrition on water flow through the apoplastic bypass in cotton roots. J Exp Bot **45:** 423–428

Steudle E (1992) The biophysics of plant water: compartmentation, coupling with metabolic processes, and flow of water in plant roots. *In* GN Somero, CB Osmond, CL Bolis, eds, Water and Life: Comparative Analysis of Water Relationships at the Organismic, Cellular and Molecular levels. Springer-Verlag, Berlin, pp 173–204

Steudle E (1993) Pressure probe techniques: basic principles and application to studies of water and solute relations at the cell, tissue and organ levels. *In* JAC Smith, H Griffiths, eds, Water Deficits: Plant Responses from Cell to Community. Bios Scientific, Oxford, UK, pp 5–36

Steudle E, Boyer JS (1985) Hydraulic resistance to radial water flow in growing hypocotyl of soybeans measured by a new pressure perfusion technique. Planta **164:** 189–200

Steudle E, Jeschke WD (1983) Water transport in barley roots. Planta **177:** 281–295

Steudle E, Murrmann M, Peterson CA (1993) Transport of water and solutes across maize roots modified by puncturing the endodermis. Plant Physiol **103:** 335–349

Tanton W, Crowdy SH (1972) Water pathways in higher plants. II. Water pathways in roots. J Exp Bot **23:** 600–618

Tyree MT (1968) Determination of transport constants of isolated *Nitella* cell walls. Can J Bot **46:** 317–327

Tyree MT (1969) The thermodynamics of short distance translocation in plants. J Exp Bot **20:** 341–349

Tyree MT (1973) An alternative explanation for the apparently active water exudation in excised roots. J Exp Bot **24:** 33–37

Tyree MT, Yanoulis P (1980) The site of water evaporation from sub-stomatal cavities, liquid path resistances and hydroactive stomatal closure. Ann Bot **46:** 175–193

Woehlecke H, Ehwald R (1995) Characterization of size-permeation limits of cell walls and porous separation materials by high performance size exclusion chromatography. J Chromatogr **708:** 263–271

Wooley JT (1983) Maintenance of air in intercellular spaces. Plant Physiol **72:** 989–991

Zhu GL, Steudle E (1991) Water transport across maize roots. Simultaneous measurement of flows at the cell and root level by double pressure probe technique. Plant Physiol **95:** 305–315

Zimmermann U, Rygol J, Balling A, Klöck G, Metzler A, Haase A (1992) Radial turgor and osmotic profiles in intact and excised roots of *Aster tripolium*. Plant Physiol **99:** 186–196

Zimmermann U, Steudle E (1975) The hydraulic conductivity and volumetric elastic modulus of cells and isolated cell walls of *Nitella* and *Chara* ssp.: pressure and volume effects. Aust J Plant Physiol **2:** 1–12